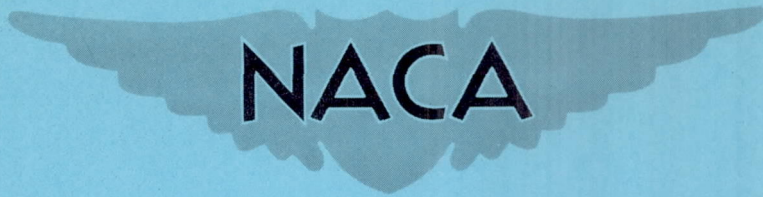


FEB 25 1958

CONFIDENTIAL

Copy 1
RM E57L18

NACA RM E57L18



RESEARCH MEMORANDUM

A PRELIMINARY STUDY OF THE EFFECT OF BORIC OXIDE DEPOSITS
ON THE PERFORMANCE OF TWO SELECTED TURBINE
STATOR-BLADE SHAPES

By Paul C. Setze and William J. Nusbaum

Lewis Flight Propulsion Laboratory
Cleveland, Ohio

CLASSIFICATION CHANGE
To *Unclassified*
By authority of *Memorandum 1-20-11151 by H. Munn*
Changed by *M. Ruda* Date *2-1-57*

CLASSIFIED DOCUMENT

This material contains information affecting the National Defense of the United States within the meaning of the espionage laws, Title 18, U.S.C., Secs. 793 and 794, the transmission or revelation of which in any manner to an unauthorized person is prohibited by law.

NATIONAL ADVISORY COMMITTEE FOR AERONAUTICS

WASHINGTON
February 25, 1958

FILE COPY
To be returned to
the files of the National
Advisory Committee
for Aeronautics
Washington, D. C.

CONFIDENTIAL

NATIONAL ADVISORY COMMITTEE FOR AERONAUTICS

RESEARCH MEMORANDUMA PRELIMINARY STUDY OF THE EFFECT OF BORIC OXIDE DEPOSITS ON THE
PERFORMANCE OF TWO SELECTED TURBINE STATOR-BLADE SHAPES

By Paul C. Setze and William J. Nusbaum

SUMMARY

The performance of two stator-blade shapes with and without boric oxide deposits was determined in a two-dimensional cascade. The first blade had a large amount of curvature and suction-surface diffusion downstream of the throat, while the second blade had no curvature and a minimum amount of suction-surface diffusion downstream of the throat. Without deposits, the performance of the two blades was very similar. The first blade accumulated larger boric oxide deposits on the suction surface downstream of the throat than did the second blade. The results show that the boric oxide deposits caused total-pressure losses of 12 and 6 percent and decreases in the blade-exit flow angle of 6.5° and 1.5° for the first and second blades, respectively.

Separation of the flow from the suction surface of the blade is believed to have caused the large deposit buildup and the resulting performance loss measured for the first blade. It appears that a blade with no flow separation on the suction surface would show a minimum performance loss due to boric oxide deposits.

INTRODUCTION

Recent advances in the design of a turbojet-engine primary combustor for pentaborane fuel (ref. 1) have increased the chances for use of boron fuels in this component. However, several problem areas remain to be solved, the major one of these being the effect of boric oxide on turbine performance. Reference 2 points out that a large share of the performance loss observed when an engine is operated on a boron-containing fuel (such as the full-scale engine test of ref. 3) might be attributed to the turbine stator. An obvious shift in turbine performance occurs because the boric oxide (B_2O_3) deposit on the blades decreases the stator throat area. A second phenomenon that would decrease stator performance is the increase in frictional pressure drop because of the presence of

the rough boric oxide layer on the blade surfaces. The third performance shift, and probably the major reason for the over-all engine performance loss, occurs because of flow separation on the stator blade. On a number of today's turbojet engines the velocity distribution along the suction surface of the stator blade is such that diffusion of the flow occurs near the trailing edge. This diffusion, when coupled with a rather large boundary layer in this region, often leads to separation of the flow.

Large accumulations of boric oxide have been observed when flow separation occurs downstream of the leading edge of a surface (ref. 2). When boric oxide deposits on a surface, the shear stress exerted on the liquid film by the flowing gas stream induces motion of the film in the direction of gas flow. When this moving liquid film enters regions of flow separation, the shear stress drops to near zero and the film stops moving. Thus, this region is being continually supplied with liquid boric oxide that is not being removed. Eventually the deposit builds up to such a thickness that it either becomes unstable and flows off or enters the free stream and blows off. Even when removal of oxide from this region is occurring, the equilibrium thickness of boric oxide in a region of flow separation is many times thicker than in a region where the flow is attached.

If this phenomenon occurs on a stator blade, the point of flow separation probably would be forced upstream, and the tangential component of the velocity leaving the stator would be decreased so that an increase in turbine pressure ratio would be required to maintain constant turbine work. The net effect would be a decrease in engine efficiency.

This report presents the results of a two-dimensional cascade investigation of two stator-blade shapes. The objectives of the program were:

- (1) To verify experimentally the presence of large boric oxide buildups in regions of flow separation on a conventional stator blade.
- (2) To determine the effect of boric oxide deposits on stator-blade performance.
- (3) To attempt to minimize the effect of boric oxide deposits by changes in the blade profile.

The two blades were designed to have the same inlet and exit flow angles and the same solidity. One blade was designed with a curved suction surface downstream of the throat and a thick blade section. The other blade was designed with a straight suction surface downstream of the

throat resulting in a comparatively thin blade section. Previous tests (ref. 4) have shown that a curved-back blade is more susceptible to flow separation than a straight-back blade.

Total-pressure ratio and flow-angle data are presented for the blades both with and without the boric oxide deposit. The boric oxide was deposited on the blades at some predetermined test condition (a nominal inlet temperature of 1250° F and a nominal exit total-to-static-pressure ratio of 2.1). After shutdown the total-pressure and angle surveys were made at the blade trailing edge with cold air flowing through the cascade; the boric oxide remained on the blade in the frozen state. The fuel used in this investigation was trimethyl borate - methyl alcohol azeotrope (TMB).

SYMBOLS

The following symbols are used in this report:

a_{cr}	critical velocity of sound, ft/sec
c	blade chord length, ft
P	total pressure
p	static pressure
V	velocity, ft/sec
α	flow turning angle, deg
θ	boundary-layer momentum thickness, ft

Subscripts:

in	conditions at cascade inlet
out	conditions at cascade outlet

EXPERIMENTAL APPARATUS AND PROCEDURE

General Description

A diagram of the test apparatus is presented in figure 1. Combustion air from the laboratory central air system was supplied to the apparatus. The air was throttled with a remotely operated butterfly valve and metered through a standard ASME orifice. From the inlet

plenum the air entered two parallel tubular combustors in which the fuel was burned. The combustion products entered a large calming chamber where any large boric oxide particles, sheared from the combustor walls, would settle out. A two-dimensional cascade of four blades was attached directly to the downstream face of the calming chamber. The combustion products, after leaving the cascade, were directed into a pipe that was connected to the building altitude exhaust system. The open space downstream of the cascade section provided a means for photographing the deposits on the blades while a test was in progress.

Fuel System

Two almost identical fuel systems, one supplying JP-4 and one supplying TMB, were used in parallel (fig. 2). By means of an interconnection between the two systems, the TMB system was purged with JP-4 fuel after each test. Fuel flow was measured with a rotating-vane-type flowmeter.

Cascade Section

Figures 3 and 4 show the cascade section which consisted of four two-dimensional blades positioned and welded between two parallel plates. The top and bottom blades had plates welded to the leading edge, parallel to the inlet flow. The four plates made up a rectangular duct, the upstream end of which was rounded to form a smooth entry. The inlet duct extended into the calming chamber.

In an effort to obtain two-dimensional flow near the middle of each blade, the blade span was made 6 inches. This length was limited by the flow capacity of the combustors.

The deposition rate from a stream of TMB combustion products is about one-third that of pentaborane (B_5H_9) combustion products. Reference 5 shows that the equilibrium thickness is proportional to the integrated deposition rate over the surface. Therefore, the actual value of the equilibrium thickness on the blades tested with TMB would be expected to be the same as the equilibrium thickness on blades one-third their size tested with pentaborane. For this reason the blades were made about three times larger (chord equal to about 5.5 in.) than the stator blades of conventional turbojet engines.

Description of Blades Tested

The two blade profiles investigated were designed with approximately the same solidity (actual chord divided by pitch equal to 1.5) and the same amount of turning (67°).

A description of the two blade profiles tested is presented in figure 5. Blade 1 (fig. 5(a)) has a curved suction surface downstream of the throat. The blade-surface velocity distribution on blade 1 for the choked condition, as calculated by the direct stream-filament method (ref. 6), is presented in figure 6(a). The dashed-line part of the velocity distribution curves was estimated, because this part of the curve falls in the unguided portion of the flow channel and cannot be calculated by the stream-filament method. The blade-surface velocity distribution curves show a gradually increasing velocity on the blade suction surface from the inlet to a point downstream of the throat, where a critical velocity ratio V/a_{cr} of 1.20 or possibly higher is reached. From this point on the suction surface the flow must decelerate to an exit critical velocity ratio of about 1.04. Separation of the flow is apt to occur on blade 1 somewhere between the throat and the trailing edge.

Figure 5(b) presents a description of blade 2, which was designed to have the same solidity and turning as blade 1. However, this blade has a straight suction surface downstream of the throat. The velocity distribution curve (fig. 6(b)) shows a rapidly increasing velocity on the suction surface, reaching a maximum V/a_{cr} of 1.09 about one-third the length from the leading edge. Downstream of the throat the flow decelerates gradually to an exit V/a_{cr} of 1.04. The velocity distribution curves show less diffusion on the suction surface of blade 2 than on the suction surface of blade 1.

INSTRUMENTATION

The following table summarizes the instrumentation used for each test (the station numbers refer to fig. 1):

Station	Temperature	Pressure
1	One thermocouple	One static-pressure Orifice Δp
2	One thermocouple ^a	One static pressure ^a
3	Two rakes of seven thermocouples ^a	Two total-pressure rakes ^a One static pressure ^a
4	Six thermocouples	Two static pressures
5	None	Total-pressure probe ^b Angle probe ^b

^aSame instrumentation for each combustor. (Total pressure at station 4 is assumed to be equal to static pressure in calming chamber, which is measured at two positions.)

^bSurvey probes installed for cold-flow tests only.

Test Procedure

Each test was conducted in two parts. The first part consisted of burning TMB fuel in the combustors and depositing boric oxide on the stator blades. The second part consisted of the total-pressure and angle surveys at station 5, which were run with air at room temperature.

Each of the deposit tests was conducted in the following manner: When combustor-inlet air temperature had been established, combustion was initiated on JP-4 fuel. Following ignition, the air and fuel flows were adjusted to give the desired cascade-inlet temperature and total pressure. This condition was held until temperature equilibrium in the apparatus was established. At this time the output from each of the sensing instruments in the apparatus was recorded. JP-4 fuel flow was then gradually reduced, while TMB fuel flow was increased (so that temperature was held nearly constant) until only TMB was being injected into the combustor. The entire fuel changeover procedure took less than 1 minute. During the TMB portion of the test, instrument data were recorded every minute for the first 10 minutes and every 5 minutes thereafter until conclusion of the test at 30 minutes. Each test was conducted at a nominal cascade-inlet temperature of 1250° F and a nominal cascade-exit total-to-static-pressure ratio of 2.10. Motion pictures taken of the cascade showed that the character of the deposit changed very little during the shutdown procedure.

After conclusion of the deposit test, detailed total-pressure and angle surveys were made at station 5. The survey consisted of three traverses across the center blade passage and the two blade wakes on either side: one traverse at the midspan position of the blade and two traverses 1/2 inch on either side of the midspan position. The blades were surveyed at these three positions in order to average the normal differences in the deposit along the blade span. The survey probes were actuated by means of remotely operated probe actuators (fig. 3). The total-pressure surveys were made with a single-tube hook-type total-pressure probe aligned with the flow angle. The sensing element was a 0.030-inch-diameter tube flattened to an inside dimension of 0.010 inch. The probe was set to within 0.010 inch from the blade trailing edge. The angle surveys were made with a cobra-type probe that was positioned within 0.25 inch of the blade trailing edge. Each of the survey tests was made with air at about 70° F and at nominal exit total-to-static-pressure ratios of 1.16, 1.34, 1.61, and 2.10.

EXPERIMENTAL RESULTS

The experimental results are presented in figures 7 to 12. Figure 7 shows photographs of the suction surface of blades 1 and 2 after the deposition test. Data points showing the relation between the cascade

throat area (as calculated from the continuity equation) and run time are plotted in figure 8. In figure 9 the ratio of the boundary-layer momentum thickness to the blade chord θ/c at the blade trailing edge (as calculated from the total-pressure surveys by the method of ref. 7) is presented as a function of blade-exit critical velocity ratio; curves are shown for blades both with and without the boric oxide deposit. The blade total-pressure ratio (blade-exit total pressure divided by blade-inlet total pressure) is plotted as a function of the blade-exit critical velocity ratio in figure 10. This pressure ratio was calculated from the boundary-layer momentum thickness and blade geometry by using the method presented in reference 7. Figure 11 shows the decrease in angle through which the gas stream is turned because of the boric oxide deposit. This angle decrease was calculated by subtracting the turn angle with the deposit from the turn angle of the clean blade. The change in the tangential component of the absolute velocity leaving the blade was calculated from the change in turn angle and is presented in figure 12.

DISCUSSION OF RESULTS

Cascade Throat Area

Figure 8 shows that the cascade throat area changed very little during the deposition tests. This observation is contrary to previous results because any thickness of oxide on the surface would decrease the throat area. However, an examination of the dimensions of the system and the relative deposition rate of B_2O_3 from TMB combustion products provides an explanation for this experimental observation. Previous observations (ref. 8) indicate that a 1-to-3-percent reduction in throat area can be expected with pentaborane fuel. The boric oxide deposition rate from a stream of TMB combustion products is about one-third the deposition rate from a stream of pentaborane combustion products. For a given surface length the equilibrium thickness with TMB would be expected to be about one-third the equilibrium thickness with pentaborane for the same temperature, pressure, and combustor temperature rise. For this reason the blades investigated were made three times larger than conventional size. Therefore, the absolute thickness of the boric oxide deposit at the throat should be the same as on a blade one-third this size with pentaborane as a fuel. In scaling the blades, the ratio of throat perimeter to throat area was reduced to about one-third that of conventional blades. Consequently, with less deposit surface per unit throat area than on a conventional blade, there is less percentage change in throat area due to the boric oxide deposit than is observed on a conventional stator with pentaborane fuel. The amount of throat area reduction apparently was within the error of the method used in calculating the area. Consequently, the data presented on figure 8 show little or no area change with run time.

Boundary-Layer Momentum Thickness

Up to a free-stream critical velocity ratio V/a_{cr} of 0.9, the ratio of the boundary-layer momentum thickness to blade chord θ/c for both blades without the boric oxide deposit was about the same (fig. 9). However, flow separation on the suction surface of blade 1 appeared to occur for values of V/a_{cr} greater than 0.9; this was indicated by the greatly increased boundary-layer momentum thickness.

Both blades showed a large increase in θ/c because of the equilibrium boric oxide deposit (after 30 min of run time). A comparison of the blades with and without the boric oxide deposit at a free-stream critical velocity ratio of 1 shows that θ/c was 242 percent greater for blade 1 and 164 percent greater for blade 2 because of the deposits. At this condition ($V/a_{cr} = 1$, with deposits), θ/c for blade 2 is 37 percent less than for blade 1.

Total-Pressure Ratio

The plot of cascade total-pressure ratio against blade-exit critical velocity ratio (fig. 10) shows the same trend indicated by the boundary-layer momentum thickness. For values of the critical velocity ratio less than 0.99, both blades show about the same total-pressure ratio when no deposit is present. With the boric oxide deposit present on the blade surface, the total-pressure ratio is much less for both blades. At a critical velocity ratio of 1, the decrease in total-pressure ratio because of the deposits amounts to about 12 percent for blade 1 and 6 percent for blade 2.

The manner in which this decrease in total-pressure ratio (because of the boric oxide deposit) might effect the performance of an actual turbine is illustrated in the following discussion. For the purposes of this discussion, it will be assumed that the turbine has one stage, a stator total-pressure ratio of 0.960 (blade 1) or 0.964 (blade 2), a rotor total-pressure ratio of 0.422, and is operating with the stator choked at 85-percent efficiency. By substitution of the values of stator total-pressure ratio with the boric oxide deposit present (taken from fig. 10 for $V/a_{cr} = 1$) for the values without the deposit (0.960 or 0.964) the turbine efficiency can be calculated to fall to 76 percent with stator blade 1 and 80 percent with stator blade 2. These differences amount to turbine efficiency drops of 9 and 5 percent for stator blades 1 and 2, respectively.

Exit Flow Angle and Tangential Component of Velocity

Figure 11 shows that boric oxide deposits caused a 6.5° decrease in the angle through which blade 1 turns the flow stream (for $V/a_{cr} = 1$), and a decrease of only 1.5° for blade 2. This decrease in turning angle amounts to a 5.1 and a 1.3 percent decrease in the tangential component of the absolute velocity leaving blades 1 and 2, respectively (fig. 12).

At constant speed, turbine work is directly proportional to the change in the tangential component of velocity across the rotor. Therefore, at constant turbine speed and rotor-exit conditions, a 1-percent decrease in the tangential component of the stator-exit velocity would cause a 1-percent drop in turbine work.

SUMMARY OF RESULTS

The results of the performance investigation of the two different stator-blade shapes are summarized as follows:

1. Blade 1 (having a large amount of suction-surface diffusion and curvature downstream of the throat) accumulated large boric oxide deposits on the suction surface downstream of the throat, whereas blade 2 (having a small amount of suction-surface diffusion and no curvature downstream of the throat) showed a much smaller deposit accumulation.

2. The large deposits on blade 1 resulted in a 5.1-percent decrease in the tangential component of the blade-exit velocity at the choked condition. The decrease in the tangential component of velocity due to the deposit on blade 2 was 1.3 percent at the same condition.

3. The boric oxide deposits caused a large decrease in the total-pressure ratio across both blades. (This decrease was greater for blade 1, being about 12 percent at the choked condition as compared with about 6 percent for blade 2.)

CONCLUDING REMARKS

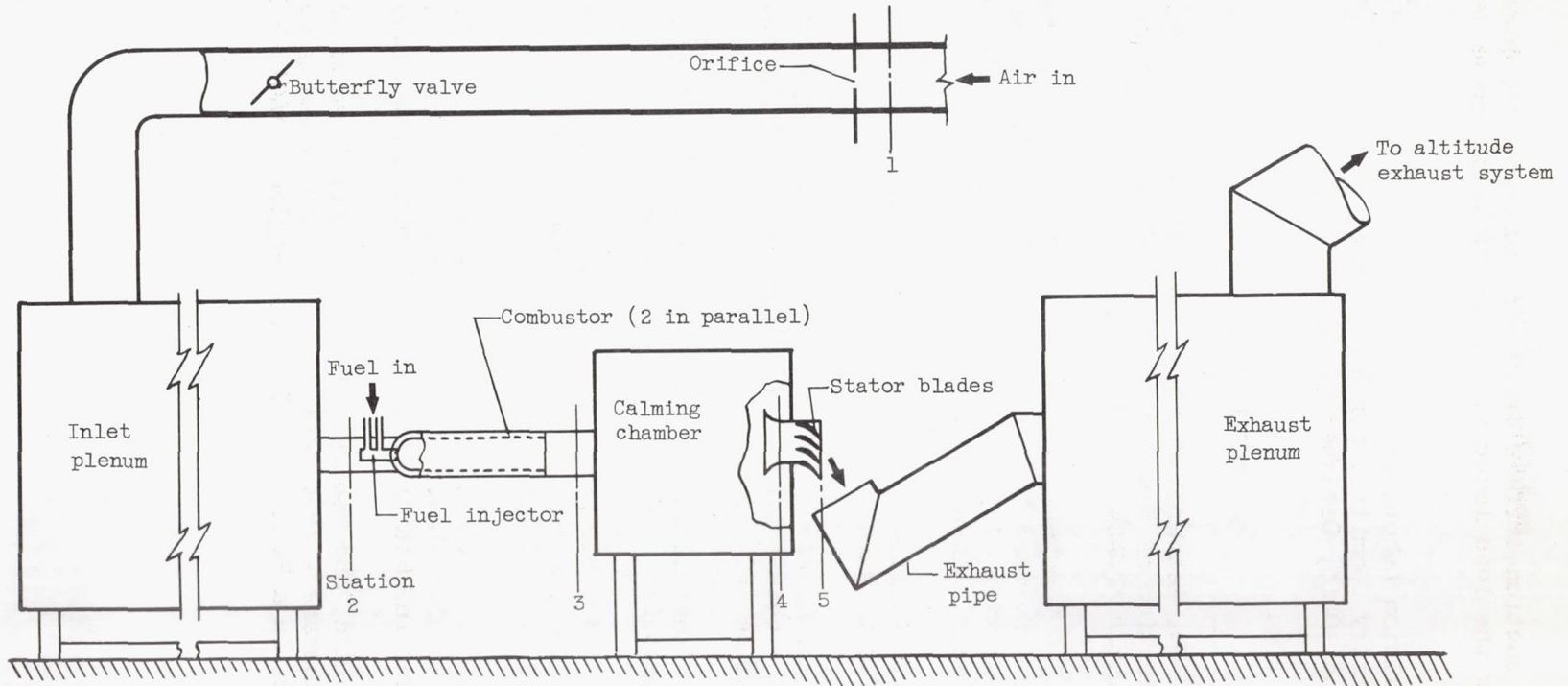
If a boron-containing fuel is to be used in the primary combustor of a turbojet engine, the performance loss associated with the deposition of boric oxide on the turbine parts must be accepted. This loss may be reduced, however, by careful design of the stator and rotor blading. The data reported herein is an attempt to establish some preliminary criteria for the design of the stator-blade shape. The results indicate that a

minimum amount of suction-surface diffusion and curvature downstream of the throat reduces the loss incurred because of boric oxide deposits.

Lewis Flight Propulsion Laboratory
National Advisory Committee for Aeronautics
Cleveland, Ohio, December 20, 1957

REFERENCES

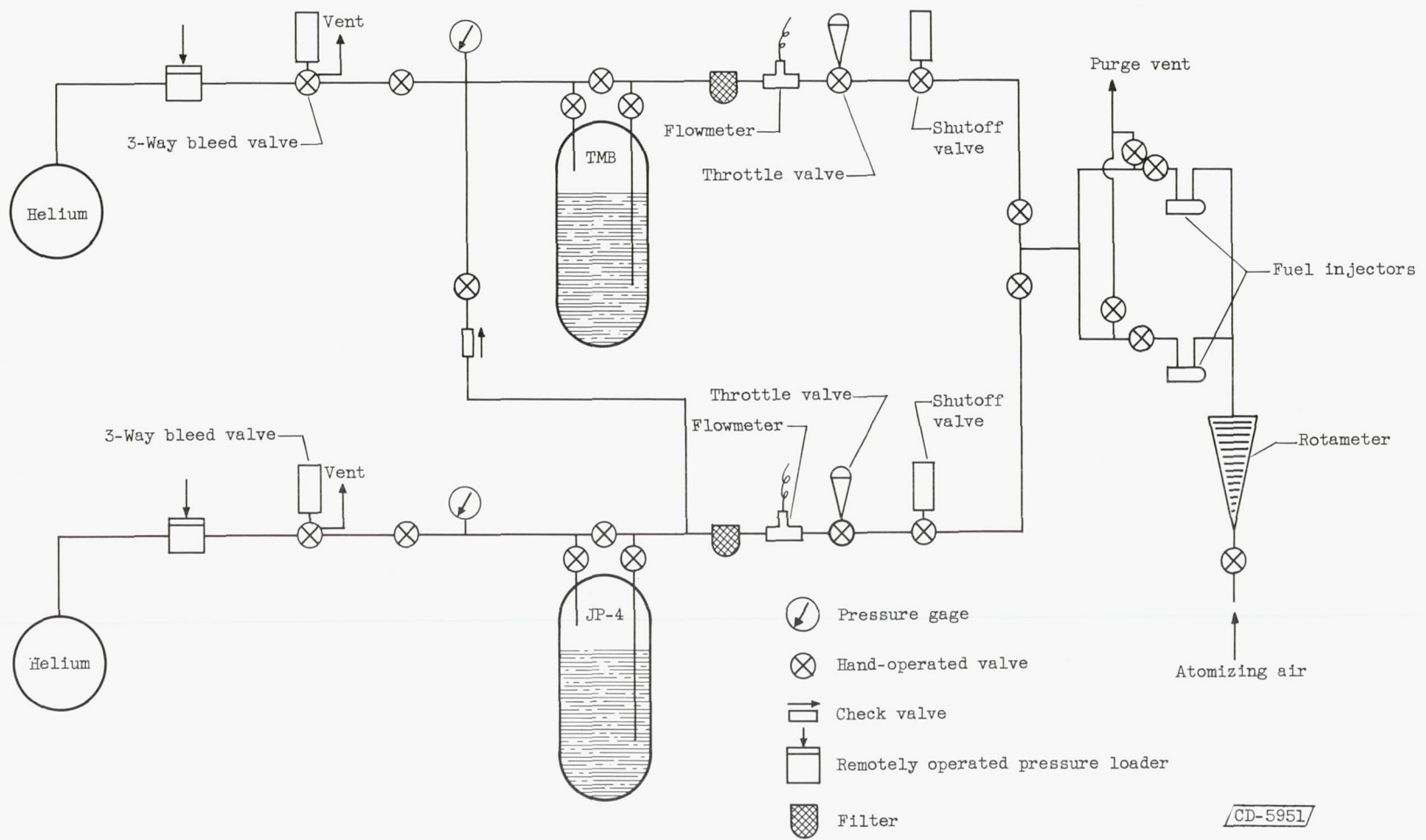
1. Kaufman, Warner B., Lezberg, Erwin A., and Breitwieser, Roland: Preliminary Evaluation of Pentaborane in a 1/4 Sector of an Experimental Annular Combustor. NACA RM E56B13, 1957.
2. Setze, Paul C.: A Theoretical and Experimental Study of Boric Oxide Deposition on a Surface Immersed in an Exhaust Gas Stream from a Jet-Engine Combustor, Including a Method of Calculating Deposition Rates on Surfaces. NACA RM E57F18, 1957.
3. Sivo, Joseph N.: Altitude Performance of a Turbojet Engine Using Pentaborane Fuel. NACA RM E57C20, 1957.
4. Ainley, D. G., and Mathieson, G. C. R.: An Examination of the Flow and Pressure Losses in Blade Rows of Axial-Flow Turbines. R. & M. No. 2891, British ARC, 1955.
5. Setze, Paul C.: Analytical Study of the Equilibrium Thickness of Boric Oxide Deposits on Jet-Engine Surfaces. NACA RM E57F13b, 1957.
6. Huppert, M. C., and MacGregor, Charles: Comparison Between Predicted and Observed Performance of Gas-Turbine Stator Blade Designed for Free-Vortex Flow. NACA TN 1810, 1949.
7. Stewart, Warner L., Whitney, Warren J., and Wong, Robert Y.: Use of Mean-Section Boundary-Layer Parameters in Predicting Three-Dimensional Turbine Stator Losses. NACA RM E55L12a, 1956.
8. Breitwieser, Roland, and Useller, James W.: Performance of Pentaborane, Pentaborane - JP-4 Fuel Mixtures, and Trimethylborate Azeotrope Fuel in a Full-Scale Turbojet Engine. NACA RM E56G19, 1956.



CD-5950

Figure 1. - Test apparatus.

CONFIDENTIAL



CONFIDENTIAL

NACA RM E57118

Figure 2. - Fuel system.

CD-5951

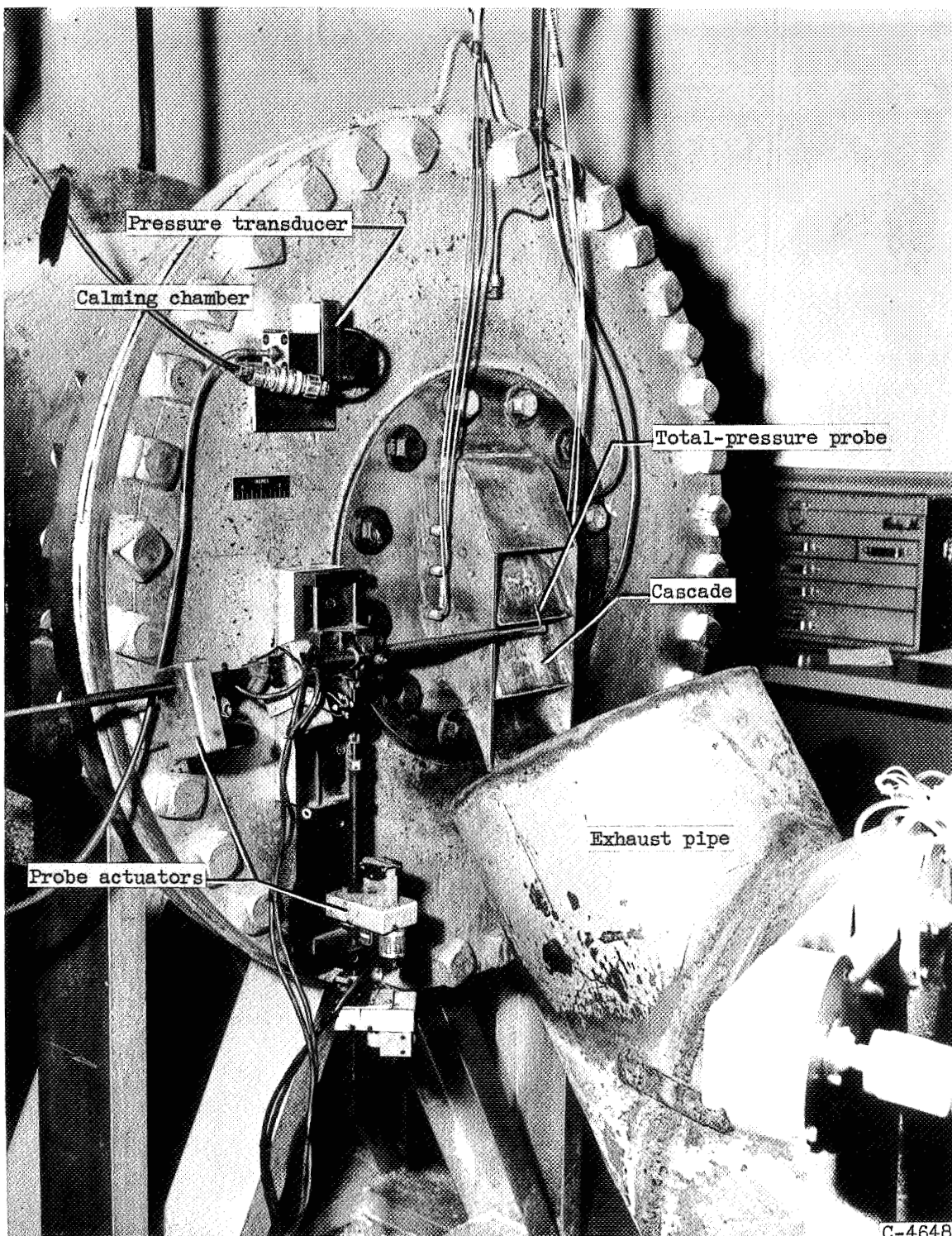


Figure 3. - Cascade mounted on calming chamber, showing probe-actuating mechanism.

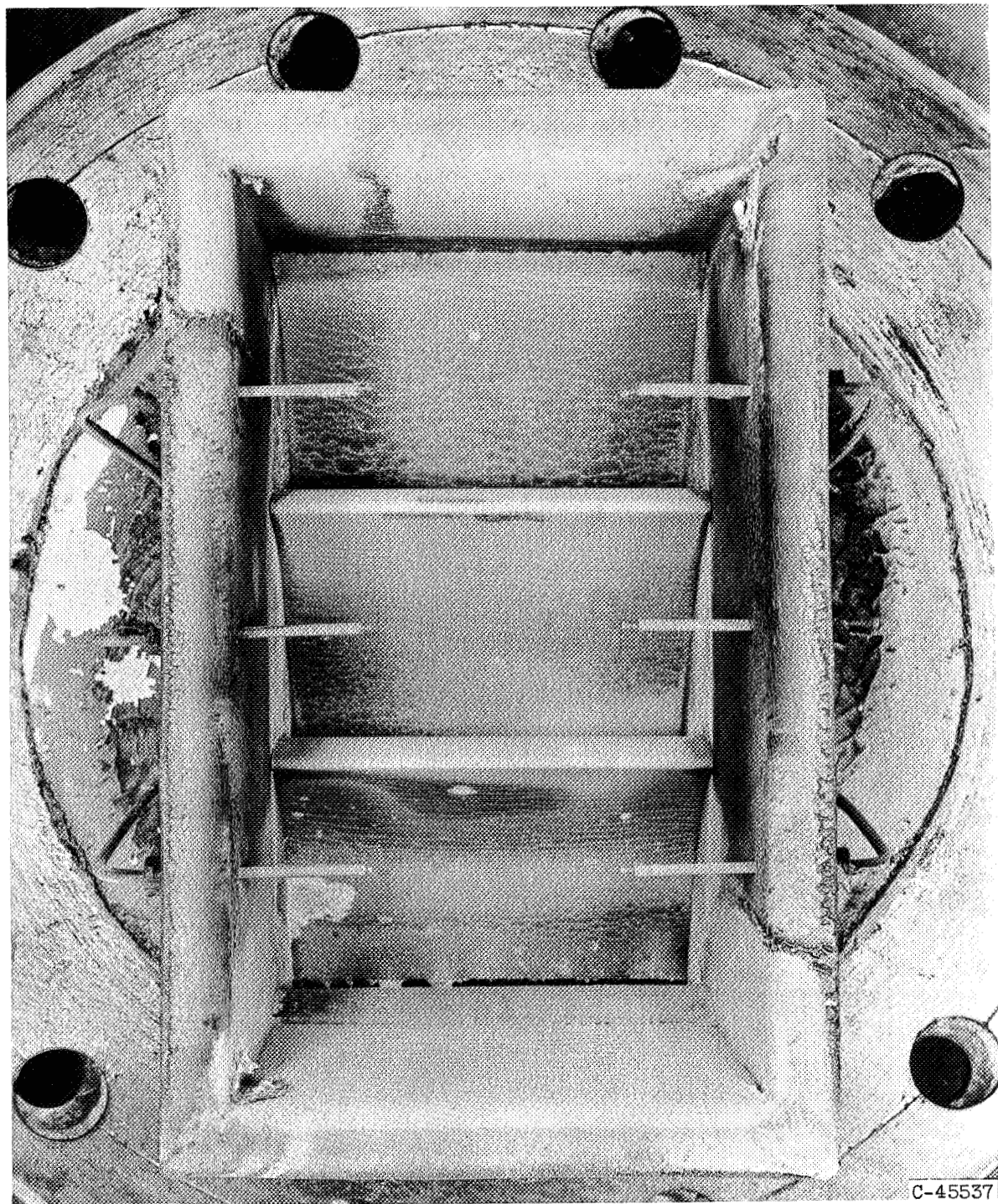
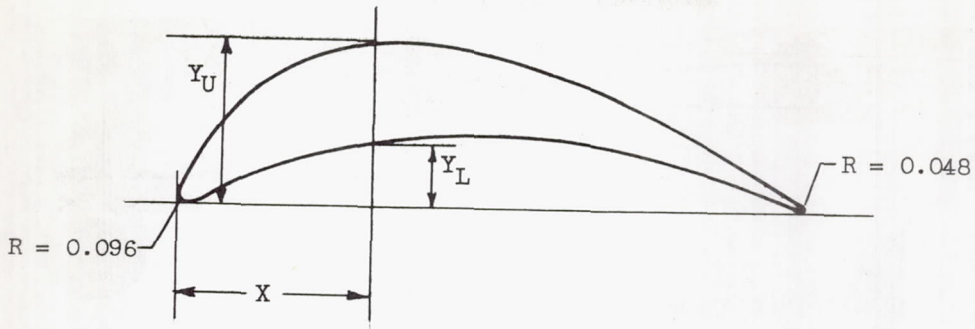
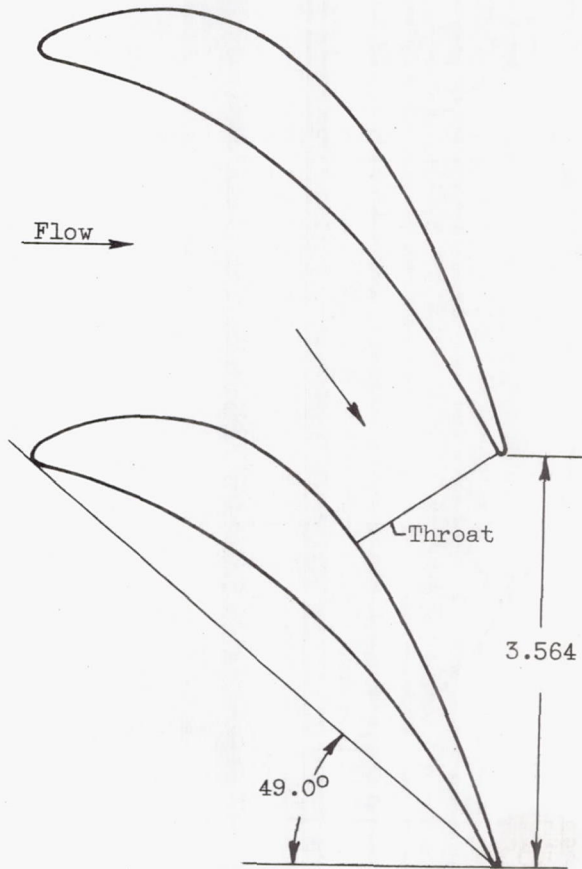


Figure 4. - Cascade-section inlet (blade 1, after 30 minutes of operation with TMB fuel).

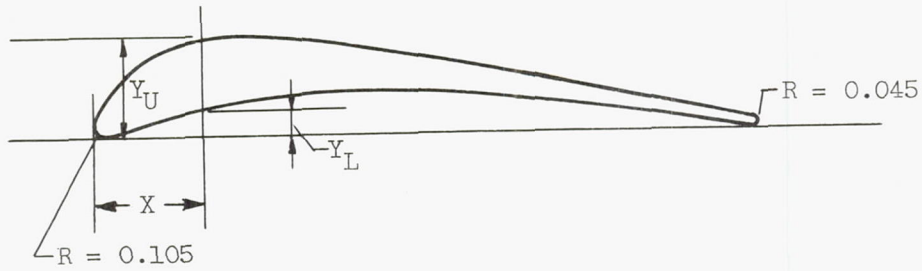


Blade coordinates		
X	Y _L	Y _U
0	0.096	0.096
.3	.096	.660
.6	.234	.984
.9	.348	1.191
1.2	.441	1.326
1.5	.510	1.401
1.8	.561	1.434
2.1	.591	1.428
2.4	.603	1.389
2.7	.603	1.326
3.0	.591	1.242
3.3	.561	1.143
3.6	.516	1.026
3.9	.456	.897
4.2	.384	.756
4.5	.297	.597
4.8	.204	.432
5.1	.096	.255
5.382	.048	.048

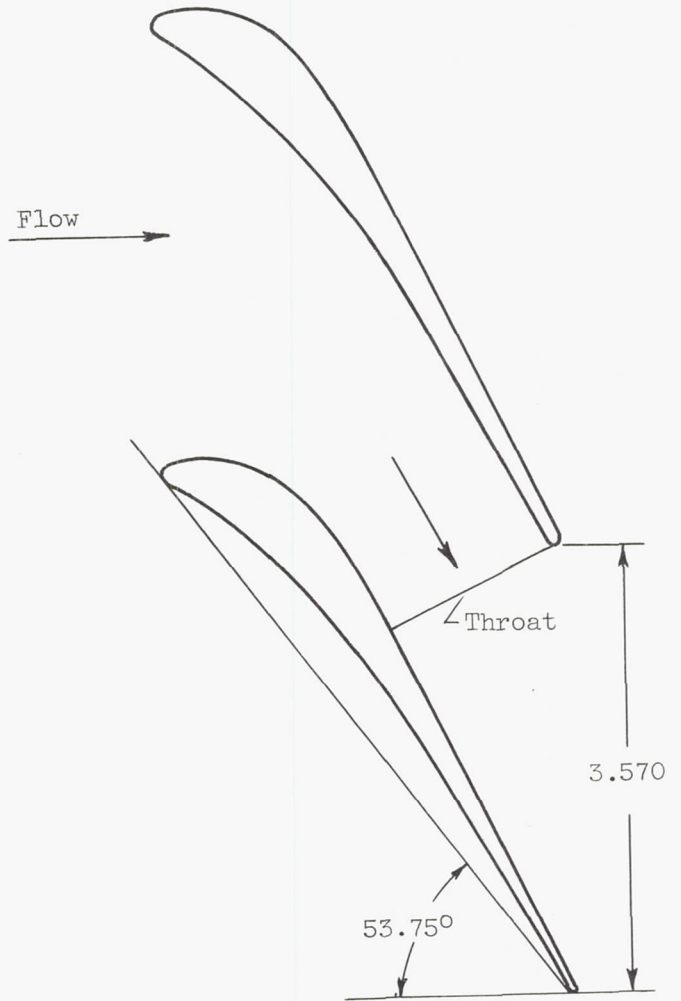


(a) Blade 1.

Figure 5. - Blade section coordinates, passage, and profile. (All dimensions in inches.)

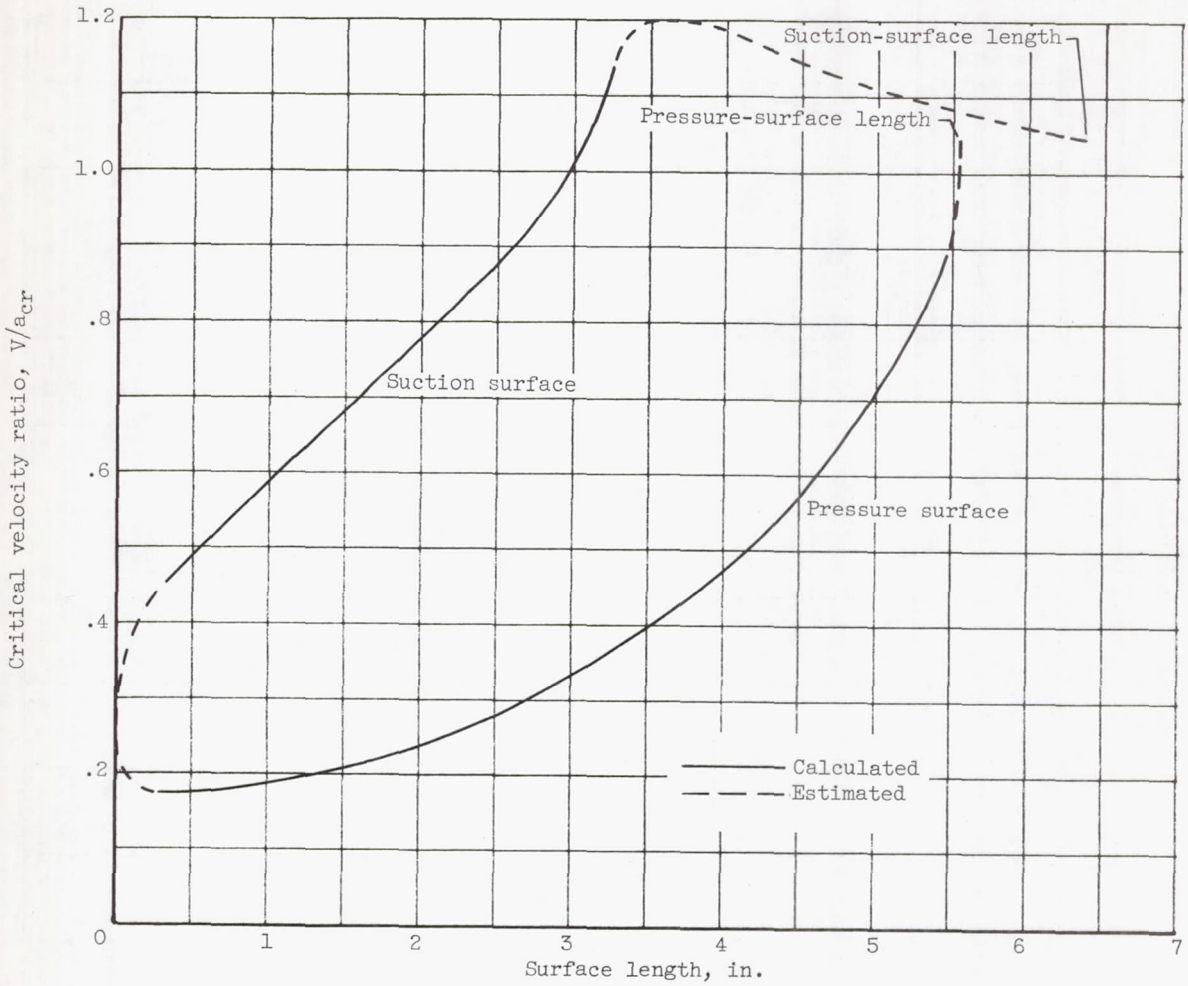


Blade coordinates		
X	Y_L	Y_U
0	0.105	0.105
.3	.063	.535
.6	.157	.723
.9	.237	.810
1.2	.297	.837
1.5	.339	.831
1.8	.363	.792
2.1	.369	.738
2.4	.364	.681
2.7	.351	.622
3.0	.328	.564
3.3	.300	.504
3.6	.264	.444
3.9	.228	.387
4.2	.186	.327
4.5	.141	.270
4.8	.093	.210
5.1	.043	.150
5.418	.045	.045



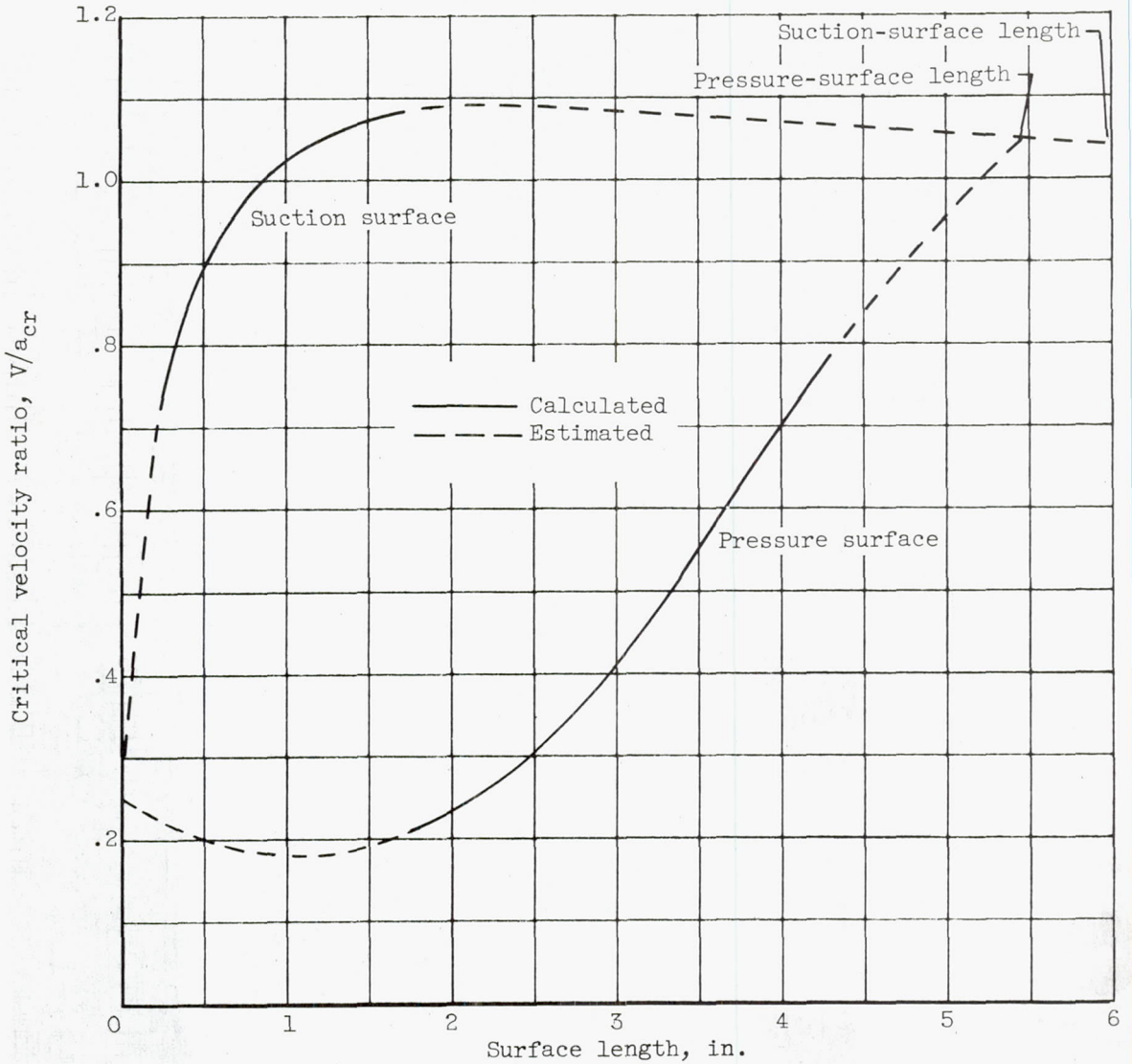
(b) Blade 2.

Figure 5. - Concluded. Blade section coordinates, passage, and profile. (All dimensions in inches.)



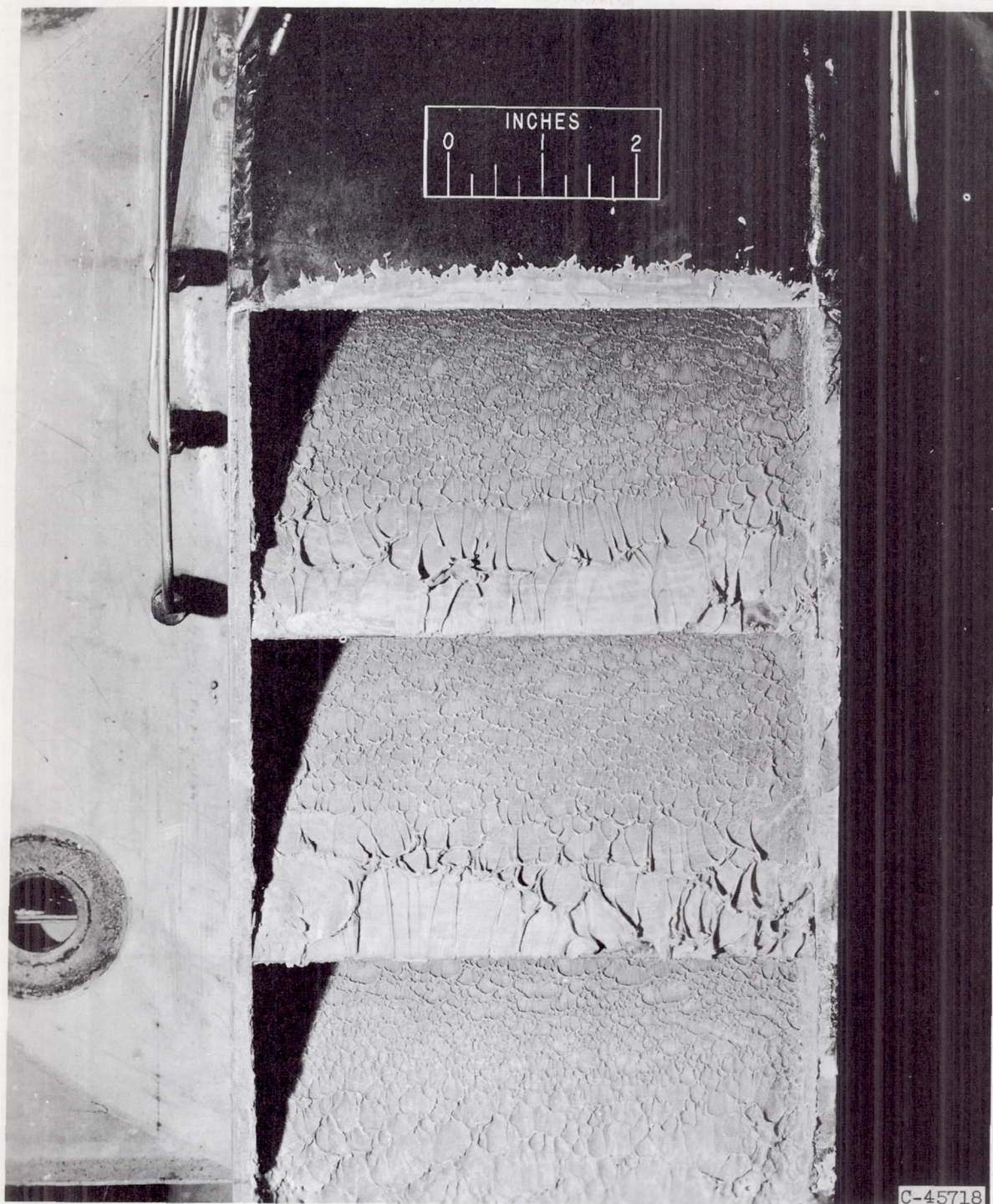
(a) Blade 1.

Figure 6. - Blade-surface velocity distribution at choked condition.



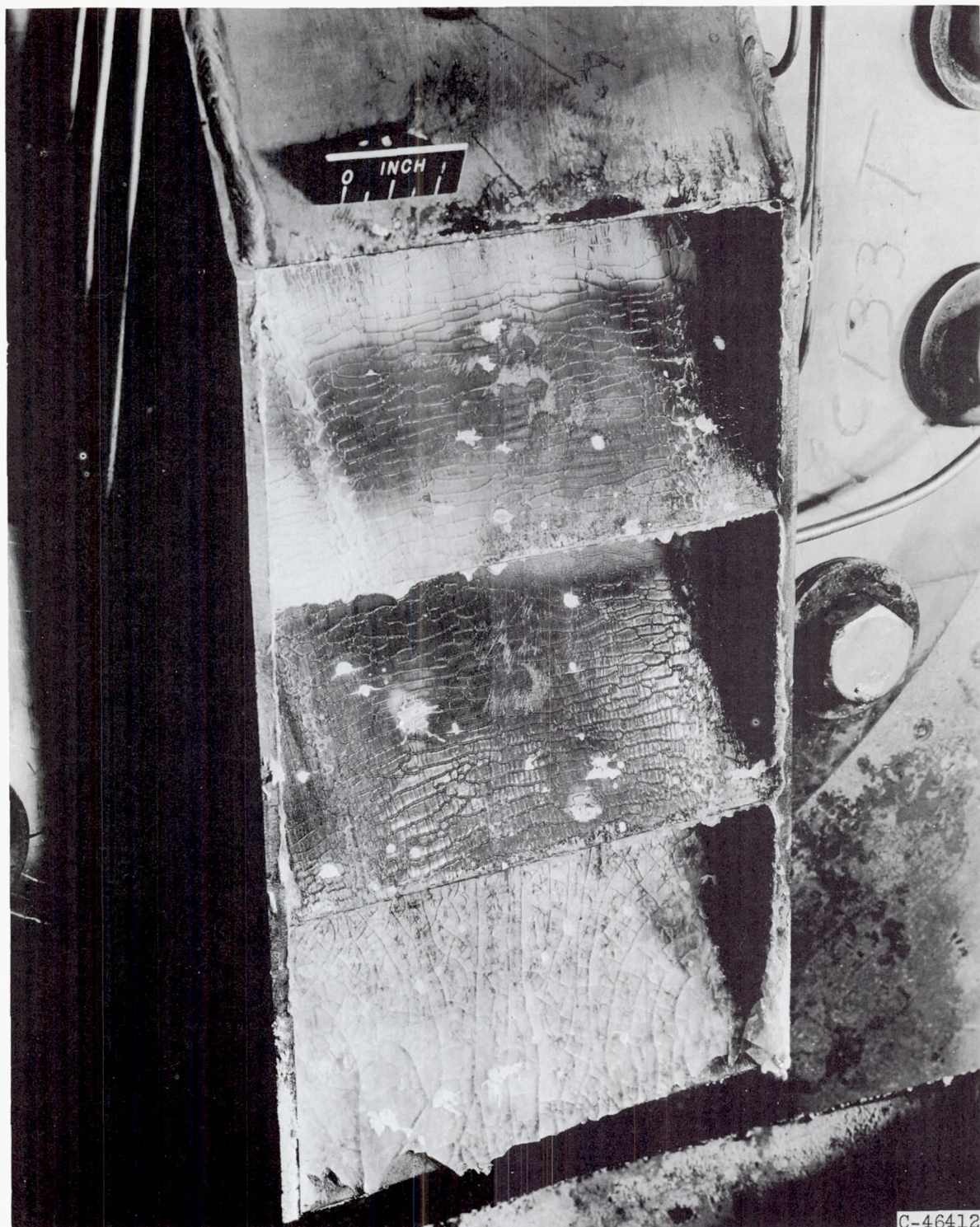
(b) Blade 2.

Figure 6. - Concluded. Blade-surface velocity distribution at choked condition.



(a) Blade 1 after 30 minutes of operation with TMB fuel.

Figure 7. - Cascade-section outlet.



(b) Blade 2 after 30 minutes of operation with TMB fuel.

Figure 7. - Concluded. Cascade-section outlet.

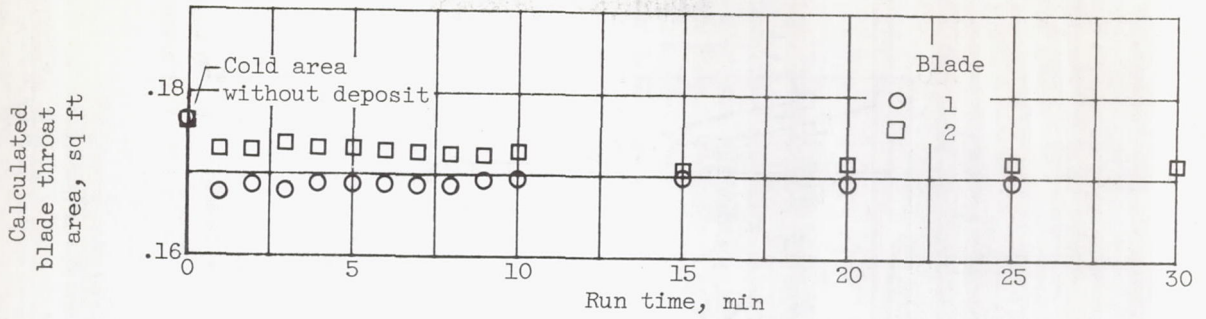


Figure 8. - Change in blade throat area with time.

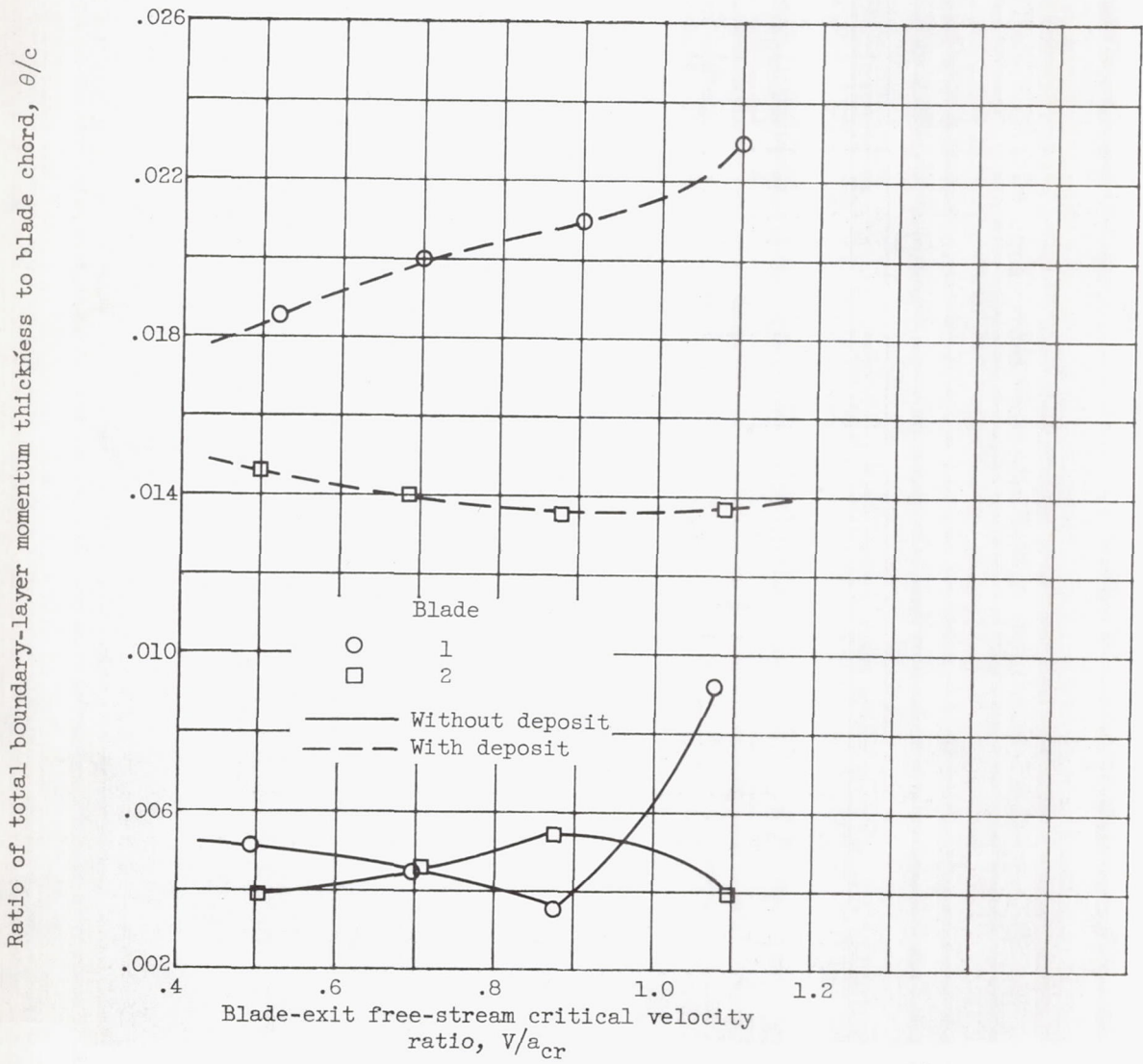


Figure 9. - Blade total boundary-layer momentum thickness with and without boric oxide deposits.

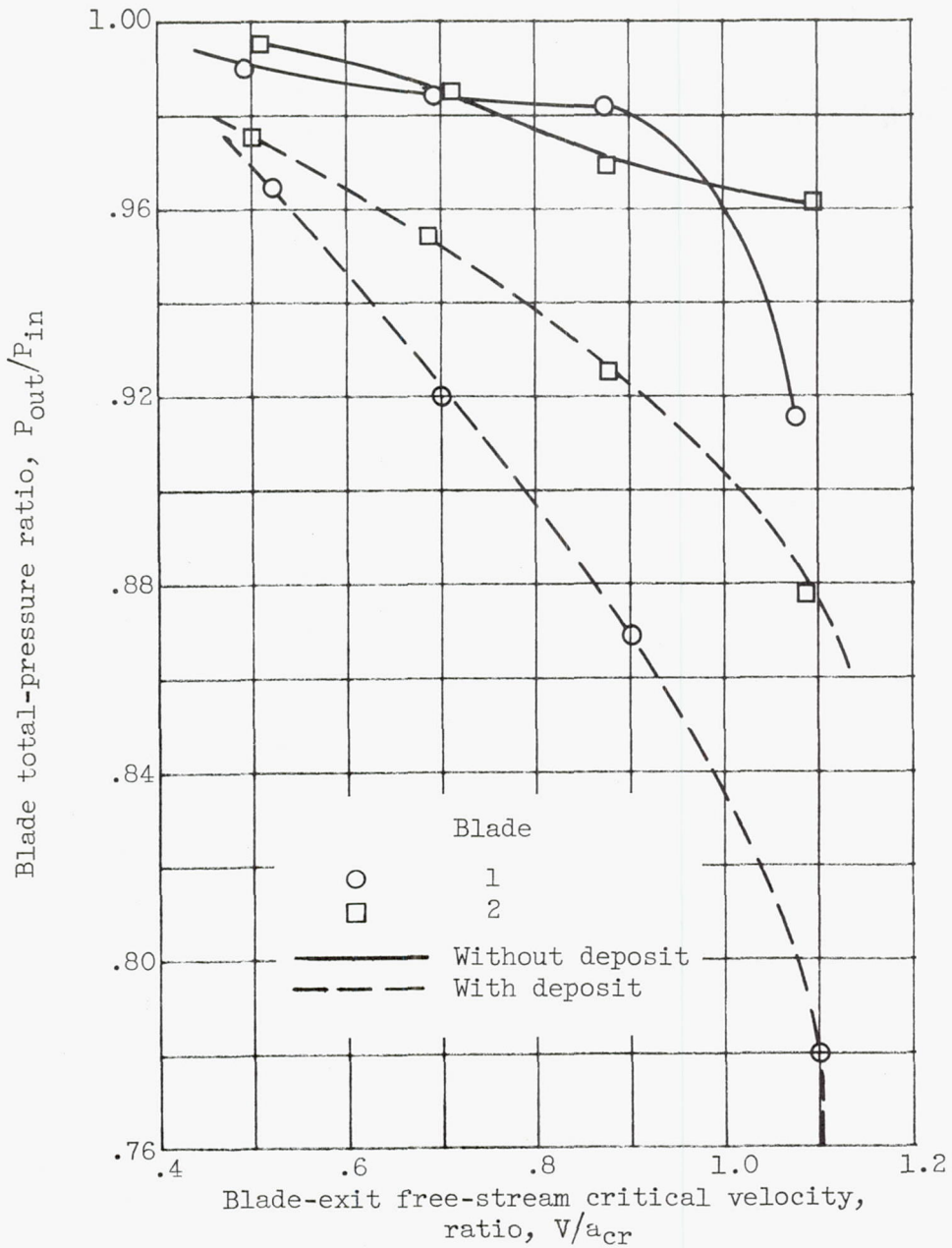


Figure 10. - Total-pressure ratio for blades with and without boric oxide deposits.

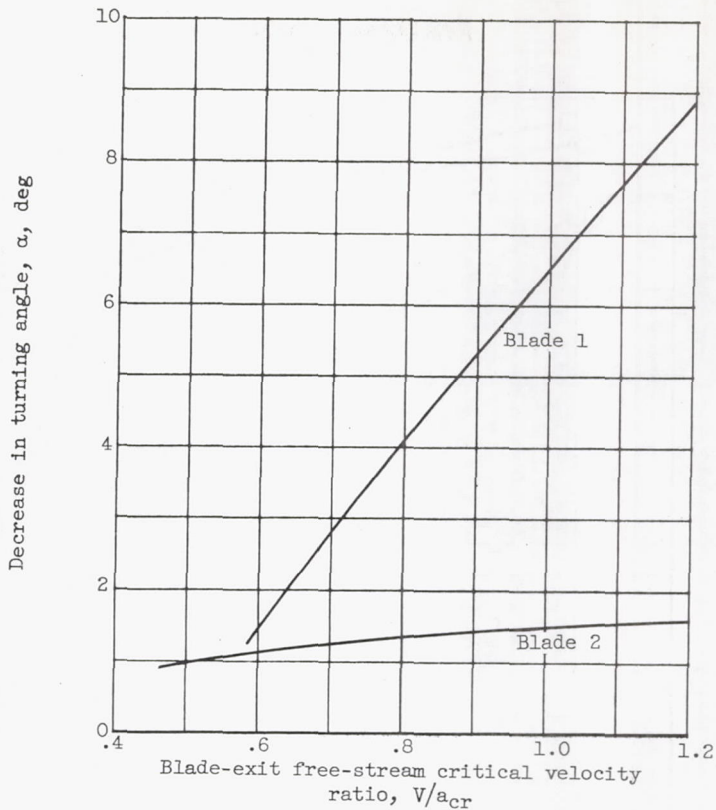


Figure 11. - Decrease in turning angle due to boric oxide deposits.

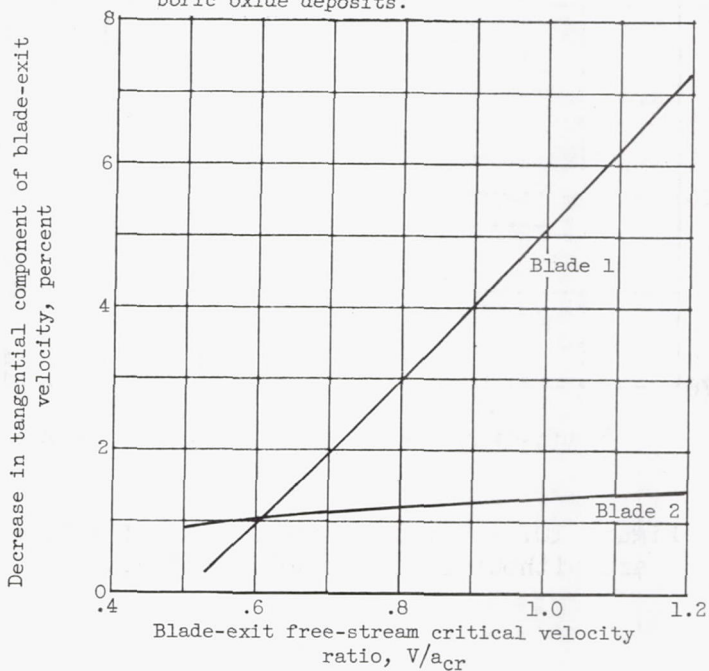


Figure 12. - Decrease in tangential component of blade-exit velocity due to boric oxide deposits.